ISUM (Idealized Structural Unit Method) Applied to Marine Structures†

Yukio UEDA* and Sherif M. H. RASHED**

Abstract

The idealized structural unit method (ISUM) has been developed to efficiently and accurately analyse the behavior of large size structures up to and post their ultimate strength. Several ISUM elements have been formulated and used to analyse the behaviour of actual large complex structures. In this paper, the basic theory and five ISUM elements are outlined and examples of recent applications to actual marine structures are presented demonstrating the effectiveness of the method.

KEY WORDS: (ISUM) (Marine Structures) (Nonlinearity) (Plastic Node Method) (Buckling) (Collapse) (Ultimate Strength)

Introduction

Despite the rapid development in the areas of non-linear structural analysis, powerful computers and CAE software, including FE mesh generators and CAD interfaces, the analysis of nonlinear behavior of a large structure by the Finite Element Method is a major job requiring extensive human resources and computer time. Unlike FEM, which requires to divide each structural component into many small elements, in the Idelized Structural Unit Method (ISUM) a structural component such as a part of a girder between two transverses, or a stiffened plate bounded by four primary supporting members is modeled by one element with only a few nodal points. Therefore, the size of the numerical problem is much reduced leading to drastic saving of human and computer resources. The nonlinear behaviour of each type of elements is idealized and expressed in the form of a set of failure functions defining the necessary conditions for different failures which may take place in the element, and a set of stiffness matrices defining the relationship between nodal force increments and nodal displacement increments before and after different failures. These elements are used in the framework of the matrix displacement method with loads applied incrementally until (and post) ultimate strength. At present, five elements are available, a deep girder element[1,2], a beam-column element[3], a joint element[4], a plate element and a stiffened plate element[5,6]. Special elements for damaged and locally buckled tubular members are also available[7,8]. ISUM has been successfully applied to analyse shiphull strength in waves[1,2,9,10], in grounding and collision[11,12], strength of offshore structures[13,14] offshore collisions[15,16] and other marine and land structural problems.

In this paper the five main available elements are briefly described, an academic example and three actual applications are presented.

Treatment of Nonlinearities in ISUM

ISUM takes account of geometric and material nonlinearities. In ISUM, geometric nonlinearity may be divided into two classes, local and global. By local geometric nonlinearity, it is referred to the nonlinear effects of large deflection and internal stresses of each element inside its boundaries regardless of the displacements of nodal points. Buckling of a plate element inside its boundaries is a typical example of this class. These local geometric nonlinear effects are included in the formulation of the stiffness equation of the ISUM elements by different methods as may be seen in the following sections. These effects are included in K_0, the small deflection stiffness matrix of an element since they do not involve large nodal displacements.

Global geometric nonlinearity is composed of those large displacement and internal stress effects directly related to nodal points displacements in the same sense as in the finite element method. These effects are essential in evaluating the behavior of slender structures and structures

† Received on May 7, 1991

* Professor

** Technical Manager, MSC Japan, Inc., Tokyo.

Transactions of JWRI is published by Welding Research Institute of Osaka University, Ibaraki, Osaka 567, Japan

having slender substructures. These effects are also included in some ISUM elements as may be seen in the following sections.

Material nonlinearity is handled by the Plastic Node Method (PNM)(17). PNM is an extention of the plastic flow theory in which nodal forces and displacements are used instead of stresses and strains. Since this method is used with all ISUM elements, it is briefly described here.

Theory of the plastic node method[17]

Basic assumptions: The plastic node method is developed by introducing a new mechanism of plastic deformation into the finite element method under the following assumptions.

(1) Plastification in an element is examined by whether or not stresses or resultant stresses at designated checking points in the element satisfy the plasticity condition.
(2) Regarding the plasticity condition, which is expressed as a function of the nodal forces, as a plastic potential and applying the theory of plastic potential, the formulation of the basic theory is performed. As a result, the plastic deformation is concentrated only at the nodes, whereas the inside of the element is always elastic. In this paper, although materials are assumed to be elastic-perfectly plastic, the effects of strain-hardening can be taken into account[18].

Elastic stiffness equation: Here, a finite element with n nodes is considered. The nodal force x and the elastic nodal displacement u^e can be represented as follows,

$$x=[x_1,x_2,\cdots,x_n]^t \tag{1}$$

$$u^e=[u_1^e,\ u_2^e,\ldots,u_n^e]^t \tag{2}$$

where x_i and u_i^e express the nodal forces and the elastic nodal displacements at the i-th node in the element, respectively. An incremental form of the elastic stiffness equation of element then can be expressed as,

$$dx=K^e du^e \tag{3}$$

where, K^e is the elastic stiffness matrix.

When the element is accompanied by large deformation, eqn(3) can be rewritten by replacing K^e by the tangential elastic stiffness matrix including the effects of geometrical nonlinearity K_t^e.

Plasticity Condition at a Checking Point and Plastic Nodal Displacement: Plastic zone in an element is examined at several designated checking points. The plasticity condition f_i at the i-th checking point can be expressed in terms of the stress components, σ_{xi}, σ_{yi}, $\cdots$, τ_{xyi}, $\cdots$ in the following form.

$$f_i(\sigma_i,\ \sigma_Y)=0 \tag{4}$$

where,

$\sigma_i=[\sigma_{xi},\ \sigma_{yi},\ \cdots,\ \tau_{xyi},\ \cdots]^t$

σ_Y; yield stress

In general, σ_i in eqn.(4) can be represented as a function of nodal force vectors at j nodes of the element. They are $x_1,\ x_2,\ \cdots,\ x_j$ ($j \leqq n$, n; the total number of element nodes). The number j depends on the displacement function assumed in the element. The plasticity condition f_i may be rewritten in the following form.

$$F_i(x_1,\ x_2,\ \cdots,\ x_j,\ \sigma_Y)=0 \ (j \leqq n) \tag{5}$$

The nodal force x_i ($i=1$ to j) can be regarded as the generalized stress. According to the theory of plastic potential, the plastic nodal displacement increment du^P is the corresponding generalized plastic strain increment and can be expressed as follows,

$$\begin{aligned} du^P &= [du_1^P,\ du_2^P,\ \cdots,\ du_j^P]^t \\ &= d\lambda_i \phi_i \end{aligned} \tag{6}$$

where, $d\lambda_i$; positive scalar

$$\phi_i=\left\{\frac{\alpha F_i}{\alpha x}\right\}=\left[\frac{\alpha F_i}{\alpha x_1},\ \frac{\alpha F_i}{\alpha x_2},\ \cdots,\ \frac{\alpha F_i}{\alpha x_n}\right]^t$$

In the vector ϕ_i, (n-j) terms vanish when the differentiation is taken with respect to the nodal forces which are not associated with the plasticity condition F_i. *Also eqn(6) shows that when the plasticity condition at checking point i* is satisfied, the resulting plastic deformation is produced at the nodes whose nodal forces are associated with the plasticity condition F_i.

Elasto-plastic stiffness equation: As a general case, it is assumed that the plasticity condition at the 1st to the k-th checking points in an element are satisfied.

Based on eqn(6), the plastic nodal displacement increment can be obtained as follows,

$$du^P=\sum_{i=1}^{k} d\lambda_i \phi_i=\phi d\lambda \tag{7}$$

where,

$\phi=[\phi_1 \phi_2 \cdots \phi_k]$

$d\lambda=[d\lambda_1,\ d\lambda_2,\ \cdots,\ d\lambda_k]^t$

As long as these k checking points in the plastic state are under loading, the following conditions must be satisfied,

$$dF_i=\phi_i^t\, dx=0 \ (i=1,\ 2,\ \cdots,\ k) \tag{8}$$

Equation (8) may be rewritten as,

$$\phi^t dx=0 \tag{9}$$

The total nodal displacement increment du is expressed by the summation of the elastic and plastic components.

$$du = du^e + du^p \tag{10}$$

Equations (3), (8), (10) and (11) may be combined and the elasto-plastic stiffness equation is finally obtained as follows,

$$dx = K^p\ du \tag{11}$$

$$K^p = K^e - K^e\phi(\phi^t K^e \phi)^{-1}\phi^t K^e$$

where

K^p; elasto-plastic stiffness matrix

Unloading may be detected by $d\lambda$ as

$$d\lambda = (\phi^t K^e \phi)^{-1}\phi^t K^e du < 0 \tag{12}$$

It is to be pointed out that in the plastic node method the elestic-plastic stiffness matrix K^p is obtained simply by matrix calculation and no integration over the element is necessary.

ISUM Elements

In the following, the five main ISUM elements are briefly described. Details of each element and assessment of its accuracy may be found in the corresponding references.

ISUM Deep Girder Element[1,2)]

The ISUM deep girder element is a prismatic part of a deep I girder with unequal flanges. Two vertical stiffeners are assumed to bound the element as shown in **Fig. 1**. These two stiffeners are assumed not to fail during loading. Further, the flanges are assumed not to buckle in a torsional mode. The element has two nodes, *i* and *j*, located at the mid-hight of each end. Axial force, bending moment and shearing force in the plane of the web are considered. Therefore, three degrees of freedom are considered at each

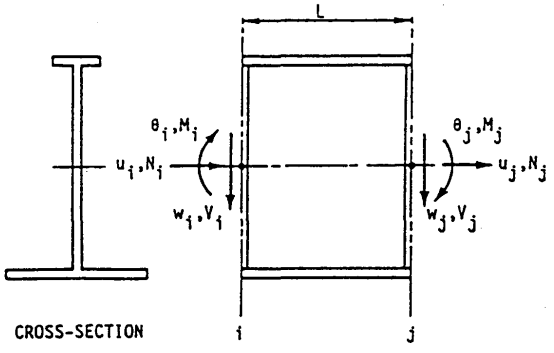

Fig. 1 The deep girder elemen, nodal points and degrees of freedom.

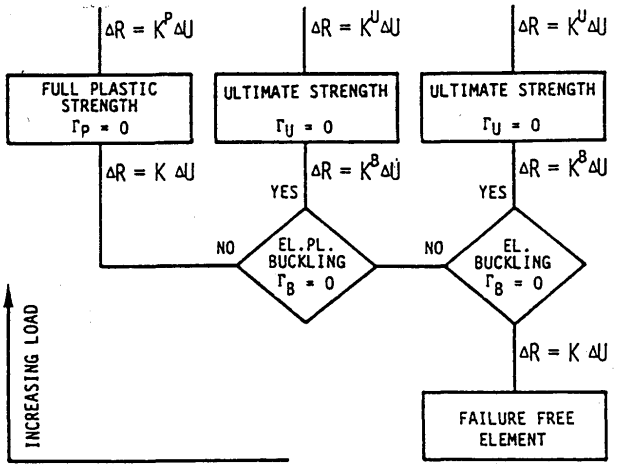

Fig. 2 Behavior of a deep girder element subjected to an increasing load.

nodal point, axial displacement u, bending rotation θ and deflection w (Fig. 1). Accordingly, the nodal displacement vector U may be expressed as follows.

$$U = [U_i U_j]^t$$
$$U_i = [u_i \theta_i w_i]^t,\ U_j = [u_j \theta_j w_j]^t \tag{13}$$

The associated nodal forces are axial force N, bending moment M and shearing force V. The nodal force vector R may then be expressed as,

$$R = [R_i R_j]^t,$$
$$R_i = [N_i M_i V_i]^t,\ R_j = [N_j M_j V_j]^t \tag{14}$$

The behavior of the deep girder element under an increasing load is illustrated in **Fig. 2**. As the nodal forces increase, the web of the element may buckle in the elastic range, or in the elastic-plastic range after yielding has started. If the web is thick enough, or if the nodal force vector is such, yielding may proceed until the element reached its full plastic strength without buckling.

Failure-free stiffness matrix: Before any local failures have taken place, the relation of the increment ΔR of the nodal force vector R to the increment ΔU of the nodal displacement vector U may be expressed in terms of a tangential stiffness matrix K as follows:

$$\Delta R = K\ \Delta U \tag{15}$$

K is evaluated based on the beam theory taking shear deflection into consideration.

Buckling condition: A condition for web buckling may be expressed with the aid of a buckling function Γ_B,

$$\Gamma_B = f_B(R) \geqq 0 \tag{16}$$

Post-buckling stiffness matrix: If eqn(16) is satisfied, i.e.

the web has buckled, the stiffness matrix relating the nodal force increments to the nodal displacement increments changes depending on the mode of web buckling. Denoting the new tangential stiffness matrix by K_B, eqn(15) may then be rewritten as;

$$\Delta R = K^B \Delta U \tag{17}$$

where, K^B is derived in Ref.(1,2).

After the web has buckled, when the shearing force is smaller than the pure shear buckling force V_{cr} (i.e. the shear buckling force when the girder is subjected to shear only), the shearing force is supported by the web, while the axial force and bending moment are supported by the flanges and the web. As the shearing force increases a redistribution of normal stress takes place by which a part of the axial force and bending moment originally supported by the web are transferred to the flanges. Considering this stress redistribution and the effectiveness of the web after buckling a post-buckling stiffness matrix K^{B1} is derived. Once the shearing force exceeds the pure shear buckling force, the web is assumed to sustain no normal stresses. The increments of the compressive force and bending moment are supported by the flanges only. The increments of shearing force are supported by a tension field developed in the web. In this case, the stiffness matrix K^{B2} *is similar in form to* K, however, effective section properties are used.

Ultimate strength condition: The element may continue to carry further loading until it reaches its ultimate strength. Again, a condition for ultimate strength may be represented by an ultimate strength function Γ_u,

$$\Gamma_u = f_u(R) = 0 \tag{18}$$

Here, ultimate strength is also dependent upon the value of the shearing force V. When $V \leqq V_{cr}$, post-buckling stress distributions are established for different load combinations. Ultimate strength in a certain combination is considered to be reached when at least a flange and the adjacent web fiber yield. When $V \geqq V_{cr}$ ultimate strength is assumed to be reached at collapse of a flange under axial force, caused by axial force and bending moment acting on the element, and lateral load caused by the tension field in the web, or yielding of the web under the effect of the tension field.

If the web does not buckle, the element may reach its full plastic strength. The fully plastic strength condition may be expressed as follows.

$$\Gamma_P = f_P(R) = 0 \tag{19}$$

the fully plastic strength of a cross-section is evaluated by integrating the fully plastic stress distribution over this section.

Elasto-Plastic Stiffness Matrix: When the ultimate strength condition (or the fully plastic strength condition) is satisfied at a nodal point, a plastic node is inserted at this node and an elasto-plastic stiffness matrix K^U(or K^P) is derived as shown in the previous section.

$$\Delta R = K^U \Delta U \tag{20}$$

K^e which appears in the expression of K^P in the previous chapter is K, K^{B1} or K^{B2} *depending on the state of the element.*

ISUM Tubular Beam-Column Element[3]

The ISUM Tubular Beam-Column element is a prizmatic circular tube. Six degrees of freedom are considered at each of two nodal point i and j located at the ends of the element as shown in **Fig. 3**. Nodal displacement and force vectors, U and R may be expressed as

$$U = [U_i U_j]^t,\ R = [R_i R_j]^t \tag{21}$$

where

$$U_k = [u_{xk},\ u_{yk},\ u_{zk},\ \theta_{xk},\ \theta_{yk},\ \theta_{zk}]^t,\ k = i, j$$

$$R_k = [P_{xk},\ P_{yk},\ P_{zk},\ M_{xk},\ M_{yk},\ M_{zk}]^t,\ k = i, j$$

$[\ ]^t$ = transposed matrix of $[\ ]$

A distributed lateral load q is taken into consideration.

Elastic stiffness matrix: In order to accurately deal with the geometrical nonlinearity using one element to model one whole member, an exact solution of the displacement along the element should be used.

Before buckling or yielding, the elastic large deflection behavior of the element is dealt with as a beam-column and may be expressed by the following differential equations:

$$\frac{d^4 w_y}{dx^4} + k^2 \frac{d^2 w_y}{dx^2} = \frac{1}{EI} q_y$$
$$\frac{d^4 w_y}{dx^4} + k^2 \frac{d^2 w_y}{dx^2} = \frac{1}{EI} q_z \tag{22}$$

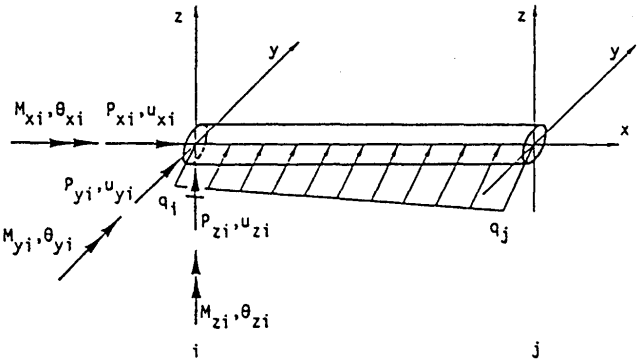

Fig. 3 The tubular beam-column element.

where,

w_y and w_z = lateral deflections in the xy and zx planes

p^y = internal axial force (compression is positive)

$k=(P/EI)^{1/2}$ is a common variable in the two equations

E = Young's modulus

I = cross-sectional moment of interia

q_y and q_z = components of the lateral load q in y and z directions

The above two equations may be solved independently. The general solution of the first of eqn(22) may be written as

$$w_y = a\cos kx + b\sin kx + cx + d + f(q_y) \tag{23}$$

$f(q_y)$ is dependent on the distribution of the lateral load q_y. The constants of integration a, b, c and d are determined from the boundary conditions at nodal points i and j, in terms of the nodal displacement U. Based on this displacement function, the relationship between nodal force R and nodal displacement U may be obtained.

The bending moment M_z and axial force P_x may be expressed as

$$M_z = -EId^2 w_y/dx^2 \tag{24}$$

$$P_{xi} = -P_{xj} = EA(u_{xi} - u_{xj} - u_b)/L \tag{25}$$

where

u_b = the axial shortening due to bending of the element (see Ref.(3))

Neglecting small terms of higher order, an increment of the nodal force dR may be expressed as follows.

$$dR + dQ = K\ dU \tag{26}$$

where

K = the tangential stiffness matrix

dQ = a load vector associated with the distributed load applied on the element

The explicit forms of K and dQ are given in Ref.(3).

It is to be noted that the effect of the lateral load appears not only in dQ, but also in K. Since, the exact solution, eqn(23), of the large deflection differential equations is employed as the displacement function of the element, the effect of elastic large deflection is taken into account.

Ultimate strength: The nodal force-displacement relationship, eqn(26) holds until the element buckles and/or yielding starts. After yielding has started, even locally, the stiffness of the element decreases. However, eqn(26) is assumed to hold in the analysis until the element buckles, or one or more full plastic cross sections are developed.

In the following, the conditions of the buckling strength and the full plastic strength of a cross section are represented and the ultimate strength condition is constructed as a combination of these.

Considering buckling strength, since one member is modeled by one element, initial out-of-straightness and residual stresses may not be explicitly considered. These have no effect on the full plastic strength of cross-sections. However they have an effect on buckling strength, which may be taken into account by using a suitable column curve. In this study, one of these presented in Ref.(19) is used. The buckling condition may then be represented in terms of a buckling function Γ_B as,

$$\Gamma_B = P - P_B = 0 \tag{27}$$

In the case of three dimensional frame structures, determination of the plane of minimum restraint and the buckling configuration requires a complicated and time consuming process. However, the restraining stiffness at nodal points i and j about y and z axes may be obtained from the global tangential stiffness matrix and then the effective buckling length may be determined (20).

In evaluating the full plastic strength, the effect of shearing stresses on plastic strength is assumed to be negligible. Therefore, the internal shearing forces P_y and P_z, and the internal twisting moment M_x do not affect the full plastic strength interaction relationship. This is expressed by the fully plastic strength function Γ_P as,

$$\Gamma_P = (\,|\sqrt{M_y^2 + M_z^2}\,|\,/M_P) - \cos\,P\,/2P_P = 0 \tag{28}$$

where

M_P = the fully plastic bending moment of the cross-section

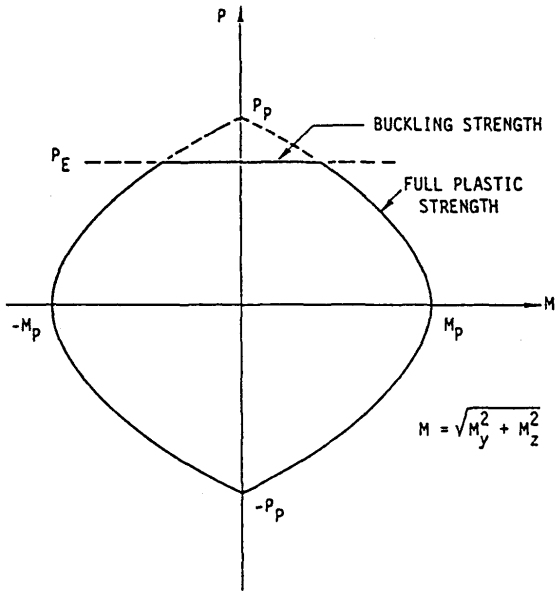

Fig. 4 Ultimate strength interaction relationship.

P_p^p = the fully plastic axial force of the cross-section

Equation (28) may be represented as shown in **Fig. 4.**

Depending on the mechanical properties of the element and the nature of the increasing load vector applied on it, it reaches either the buckling strength, or the plastic strength.

The assembly of these conditions represents the ultimate strength function Γ_u of the tubular element as shown in Fig.4.

$$\Gamma_u = \Gamma_B \text{ or } \Gamma_u = \Gamma_P \tag{29}$$

Elasto-plastic stiffness matrix: As the load increases, the ultimate strength condition, (buckling or full plastic strength) may be satisfied at nodal point 1, nodal point j and/or the location of maximum bending moment along the element. The following three cases are considered.

(a) First, let an element in which eqn(29) is satisfied at nodal points *i* or/and *j* be considered. A plastic node[17] is inserted there. Equation (29) is regarded as a plastic potential and the elestic plastic stiffness metrix is derived as shown in the section of plastic node method.

(b) If the condition of ultimate strength is satisfied at point a, which is the position of maximum bending moment along the length of the element, the element is divided at this position into two beam-column elements, ia and aj. A plastic node is inserted at point a on either element ia or element aj. Considering the condition of nodal points *i* and *j*, elastic or elasto-plastic stiffness matrices and distributed load vectors are evaluated for the two elements. Then the extra nodal displacements at point a are eliminated in the normal way.

(c) If the magnitude of the axial compressive force reaches that of buckling, the element is allowed to buckle. The axial force being maintained at the buckling load, the bending moment increases due to the increase of deflection until eqn(29) is satisfied at one or both ends and/or any point along the element's length, where a plastic node is then inserted as in (a) and/or (b).

ISUM Joint Element[4]

In the analysis of framed structures, members are usually assumed to be connected rigidly to each other at nodal points.

However, in a tubular frame with simple (unstiffened) joints, the joint may exhibit considerable flexibility in the elastic as well as the elasto-plastic ranges. These may cause excessive deflections and different internal force distribution in the structure. To take these into account, one most conventional method is to use shell finite elements for joint cans and beam elements for the members. This treatment introduces and excessive number of elements and nodes which require enormous time for modelling and computation.

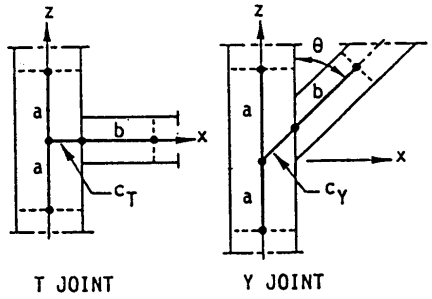

Fig. 5 Modeling T and Y joints by line elements.

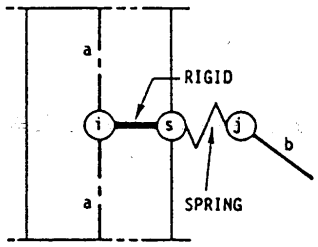

Fig. 6 Idealized Y joint element.

In order to overcome this difficulty, in the scope of the "Idealized Structural Unit Method (ISUM)", a joint element with elasto-plastic behavior has been developed[4]. Joint models for T, Y, TY, K, and V joints have been proposed based on this element. Here, the single joint model, for T and Y joints, is described.

T and Y joints are modeled by a group of elements a, b, and c_T or c_Y as shown in **Fig. 5**. Elements a and b represent the cord and brace respectively and element c_T or c_Y are joint elements to take account of wall deformation.

A joint element has 3 nodes i, s and j as shown in **Fig. 6**. The portion i-s is a rigid body and s-j is an elasto-plastic spring with a length equal to zero. Each node has 6 degrees of freedom. Nodal displacements and forces may be expressed by eqn(21) where $k = i, s, j$.

Elastic stiffness matrix: Before yielding the stiffness equation of the spring s-j may be written as

$$\begin{Bmatrix} R_s \\ R_j \end{Bmatrix} = K_s \begin{Bmatrix} U_s \\ U_j \end{Bmatrix} \tag{30}$$

where K_s = translational and rotational stiffness matrix of a spring.

U_s and R_s may be expressed in terms of U_i and R_i thus omitting the excessive internal node s as follows.

$$\begin{Bmatrix} U_s \\ U_j \end{Bmatrix} = \begin{pmatrix} t & o \\ o & I \end{pmatrix} \begin{Bmatrix} U_i \\ U_j \end{Bmatrix} = T_s \begin{Bmatrix} U_i \\ U_j \end{Bmatrix} \tag{31}$$

$$\begin{Bmatrix} R_s \\ R_j \end{Bmatrix} = \begin{bmatrix} t & o \\ o & i \end{bmatrix} \begin{Bmatrix} R_i \\ R_j \end{Bmatrix} = T_s \begin{Bmatrix} R_i \\ R_j \end{Bmatrix} \quad (32)$$

where,

t = transformation matrix

I = unit matrix

The stiffness equation of the joint element may then be derived as

$$R = K\ U \quad (33)$$

where

$R = [R_i\ R_j]^t$, $U = [U_i\ U_j]^t$

$K = T^t\ K_s\ T$ = elastic stiffness matrix

The explicit expression of K_s may be found in Ref.(4).

Joint yield condition: The yield condition of a joint is expressed in terms of axial force P acting in the joint element, moment M acting at node j and axial force P_c acting in the chord. Other internal force components are usually small enough to be neglected.

$$\Gamma_P = f(P,\ M,\ P_c) \quad (34)$$

where

Γ^P is a yield function.

Elasto-plastic stiffness matrix: When the components of internal force in element c_T or c_Y satisfy the plasticity condition

$$\Gamma_P = 0 \quad (35)$$

a plastic node is inserted at j and the stiffness equation is expressed in an incremental form as,

$$dR = K^P\ dU \quad (36)$$

where K^P = elasto-plastic stiffness matrix

The explicit form of this matrix is the same as that of case (b) in Appendix II of Ref.(3).

In a similar way, a joint model for K joint has been proposed as shown in **Fig. 7**. In this model, in addition to rigid elements and elasto-plastic elements, a beam element is introduced to express the interaction between the two braces.

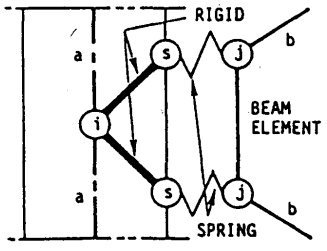

Fig. 7 Idealized K joint element.

ISUM Rectangular Plate Element[5,6,21]

The element is a rectangular plate as shown in **Fig. 8**. Its edges are assumed to remain straight after deformation. It has four nodes, one at each corner. Bending stiffness of the element is assumed to be negligible in comparison with the bending stiffness of the whole structure. Therefore, the element is treated as a membrane, Each node has three translatory degrees of freedom. Nodal displacements and forces are expressed as follows.

$$U = [U_1\ U_2\ U_3\ U_4]^t,\ U_i = [u\ v\ w]^t \quad (37)$$

$$R = [R_1\ R_2\ R_3\ R_4]^t,\ R_i = [R_{xi}\ R_{yi}\ R_{zi}]^t \quad (38)$$

Inplane biaxial and shearing forces as shown in **Fig. 8** are considered. In absence of initial imperfection, and under increasing load the element behaves as shown in **Fig. 9**. The relationship between U and R may be expressed incrementally as follows.

$$dR = K\ dU \quad (39)$$

K is evaluated depending on the state of the element.

Failure-free stiffness matrix: Before buckling, membrane strains are assumed to be linearly distributed, which

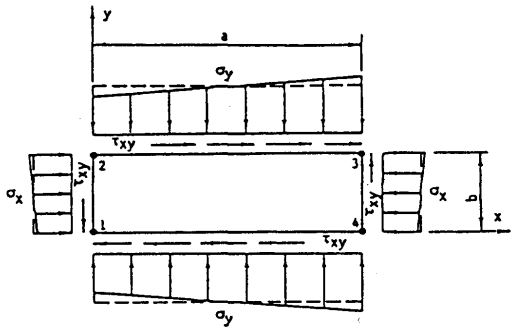

Fig. 8 Rectangular plate element.

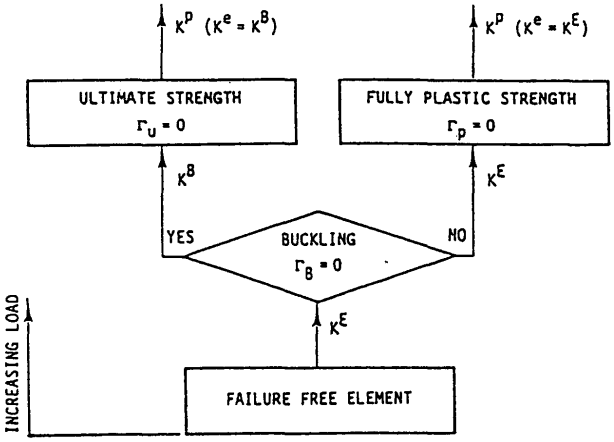

Fig. 9 Local behavior of rectangular plate element.

is reasonable for a plate field in a large structure. Using the displacement functions shown below, a stiffness matrix is derived in the same way as in the finite element method, taking global large deflection effects into consideration.

$$\begin{aligned} u &= a_1 + a_2x + a_3y + a_4xy + (b_4/2)(b^2 - y^2) \\ v &= b_1 + b_2x + b_3y + b_4xy + (a_4/2)(a^2 - x^2) \\ w &= c_1 + c_2x + c_3y + c_4xy \end{aligned} \quad (40)$$

$$K = K^E = \int (B^T\ DB\ +\ G^T\ \sigma G)\ dvol. \quad (41)$$

where B is the strain-displacement matrix (3×12) obtained using large deflection strain expressions and D is the stress-strain matrix in plane stress condition (3×3).

Buckling condition: Buckling takes place when the following buckling condition is satisfied[5].

$$\Gamma_B = f(\sigma_x,\ \sigma_y,\ \tau) = 0 \quad (42)$$

where Γ_B is buckling function.

Post-buckling stiffness matrix: After buckling has taken place, strain distributions may not be assumed linear and the displacement functions given in eqns(40) are not valid any more. At this point, as shown in Ref.(5), the buckled plate is replaced by an equivalent flat plate which has linear strain distributions. Its material properties are such that it show nodal displacement increments similar to those which would be shown by the buckled plate under the same nodal force increments. These properties are expressed in an incremental stress-strain matrix D^B (3×3) as follows.

$$d\sigma = D^B\ d\varepsilon \quad (43)$$

in this way local geometric nonlinear effects (inside element boundaries) are included in D^B. Global nonlinear effects (nodal large displacements) may be considered as before buckling.

Now the displacement function given by eqn(40) may be used together with D^P to evaluate the post buckling stiffness matrix,

$$K\ =\ K^B\ = \int (B^T\ D^B\ B + G^T\ \sigma G)\, dvol. \quad (44)$$

σ in the above equation is the average membrane stress. It is to be noted that d_{13}, d_{23}, d_{31} and d_{32} in eqn(43) are non-zero terms, reflecting the interaction between normal and shear strains which occurs after buckling. D^B is dependent on the values of the acting stresses and is evaluated at each load step.

Plasticity condition: Before, as well as after buckling, knowing the nodal displacement and average stresses acting on the element, the stresses at eight designated checking points in the element are evaluated[5] and expressed in terms of nodal forces. These are used to check plasticity against the Mises Yield condition, similarly expressed in terms of nodal forces.

$$\Gamma_{yi} = f_i(R) = 0,\ i = 1,\ 8 \quad (45)$$

Elasto-plastic stiffness matrix: When the yield condition is satisfied at a check point, plastic nodes[17] are inserted at relevant nodal points. An elestic-plastic stiffness matrix is derived as shown in the section on the plastic node method. K^e which appears in the expression of K^P is K^E or K^B depending on whether buckling has occurred, K^B, or not, K^E.

Initial deflection and residual stresses: Effects of initial defection and residual stresses are included[6]. In presence of initial deflection, lateral deflection increases right from the beginning of the application of the inplane load. Strains are not linear also from the beginning. In this case an equivalent incremental stress-strain matrix of a non-deflecting plate is derived as before[6]. This matrix, naturally, depends on the value of the working stresses and is evaluated at each load step. Residual stresses are considered in two senses.

(1) Including their effect on buckling and/or out of plane deflection, by considering an equivalent initial compressive stress used when checking buckling or calculating out of plane deflections inside element boundaries.
(2) Considering them as initial stresses on which stress increments are added.

ISUM Rectangular Stiffened Plate Element[5,6,21]

The element is shown in **Fig. 10**. Its edges, similar to the plate element, are assumed to remain straight after deformation. It has n parallel and equi-spaced stiffeners and four nodes, one at each corner. It is also treated as a membrane element. Nodal displacements and forces are expressed by eqns(37) and (38). Also here, inplane biaxial

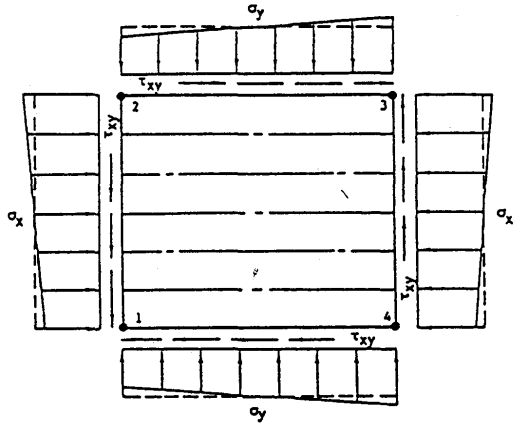

Fig. 10 Rectangular stiffened plate element.

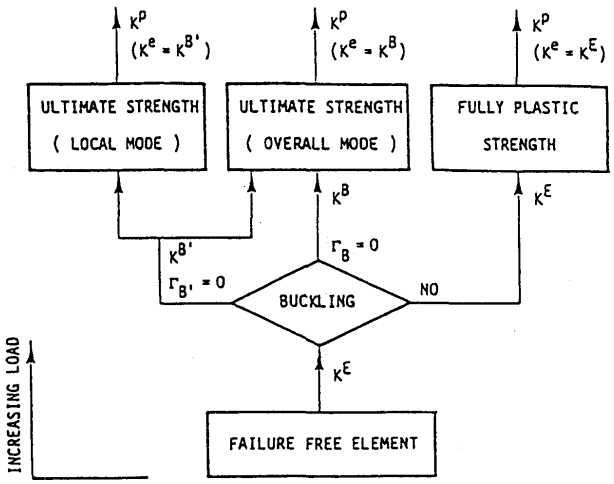

Fig. 11 Local behavior of stiffened plate element.

and shearing forces as shown in Fig. 10 are considered. In absence of initial deflection and under increasing load the element behaves as shown in **Fig. 11**. The relationship between U and R is expressed incrementally by eqn(39), where K is evaluated depending on the state of the element. In deriving the stiffness matrix K, the element is considered as an assembly of a plate and stiffnerers.

Failure-free stiffness matrix: Before buckling, membrane strains are assumed to be linearly distributed and the displacement functions, given by eqns(40) are adopted. The stiffness matrix K becomes as follows.

$$K = K^E = \int (B^t DB + G^t\ \sigma G) dvol. + \int (B_1^t E B_1 + G_1^t \sigma_{xs} G_1) dvol. \tag{46}$$

where B_1 and G_1 are the first rows of B and G matrices respectively and σ_{xs} is the axial stress in stiffeners.

Buckling conditions: Buckling may take place in an overall mode (plate and stiffeners) or local mode (plates between stiffeners) depending on which mode has a lower buckling strength. Stiffeners are assumed to be strong enough to prevent their local buckling modes. Buckling occurs when one of two buckling conditions are satisfied.

$$\Gamma_{BO} = f(\sigma_x,\ \sigma_y,\ \tau) = 0 : \text{ Overall buckling} \tag{47}$$

$$\Gamma_{BL} = f(\sigma_x,\ \sigma_y,\ \tau) = 0 : \text{ Local buckling} \tag{48}$$

Explicit forms of Γ_{BO} and Γ_{BL} are given in Ref.(5).

Post-buckling stiffness matrix: In case of eqn(47) being satisfied, overall buckling occurs. The stiffened plate is regarded as an orthotropic plate and a stiffness matrix K^{BO} is derived in a similar way as in the case of the plate element and is expressed by eqn(44). Here D^B matrix includes the contribution of stiffeners. In case of eqn(48) being satisfied, the stiffness matrix K^{BL} *becomes as follows.*

$$K = K^{BL} = \int (B^t D^B\ B + G^t\ \sigma G) dvol. + \int (B^t E B_1 + G_1^t \sigma_{xs} G_1) dvol. \tag{49}$$

Here D^B is that of a plate equivalent to the buckled plate fields and is derived as in the case of the plate element.

Plasticity condition: As in the case of the plate element stresses at eight check points are expressed in terms of nodal forces and plasticity is checked against Mises' Yield condition, similarly expressed in terms of nodal forces.

Elasto-plastic stiffness matrix K^P: The plastic node method is used as in the case of the plate element and K^P is as shown in the section on the plastic node method. Here one of K^E, K^{BO} or K^{BL} is used depending on the state of the element.

Initial deflection and residual stresses: Effect of initial defection of plate fields and residual stresses are considered in a way similar to that used with the plate element. Initial defection of stiffeners is not considered.

Examples of Application

In the following an example of a thin walled slender box column is presented to demonstrate successful interaction between local and global geometric non-linearity. Three actual applications are also presented.

Axially Compressed Box Column

A box column with a square cross-section and both ends simply supported as shown in **Fig. 12** is subjected to axial compression. Load-shortening and load-deflection curves are shown in **Figs. 13** and **14**. In the analysis, each plate field is modeled by one ISUM plate element (total 51 elements including 11 diaphragms, and 44 nodes). A small initial defection in the form of a sine curve as shown in Fig. 12 is imposed and the load applied incrementally. Two cases are analysed, the first, without taking local buckling of plate fields into account, whose results are shown by dotted lines. It may be seen that the column exhibits overall fiexural buckling with the buckling load coincidign with Euler buckling load. In the second case, local buckling of plates is taken into account. As local buckling occurs, inplane tangential stiffness of plates is reduced to one half of its original value and the overall

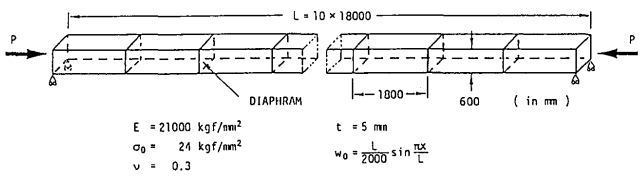

Fig. 12 Example box column and applied load.

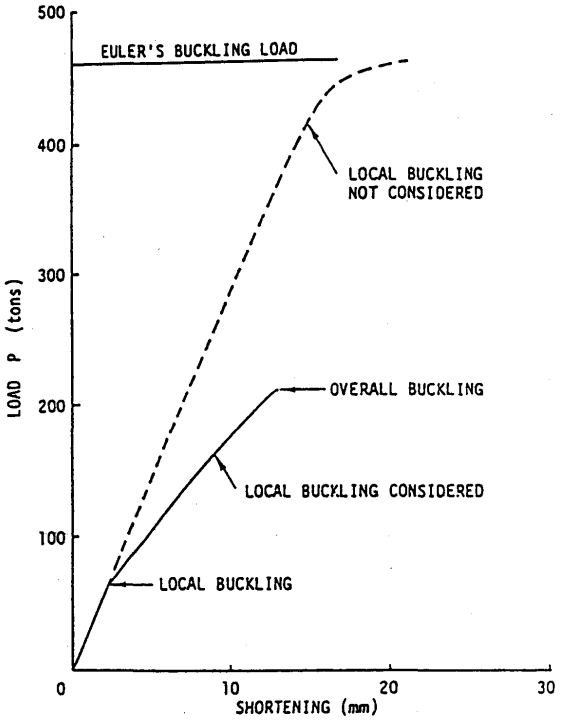

Fig. 13 Load-shortening curves of example box column subjected to axial compression.

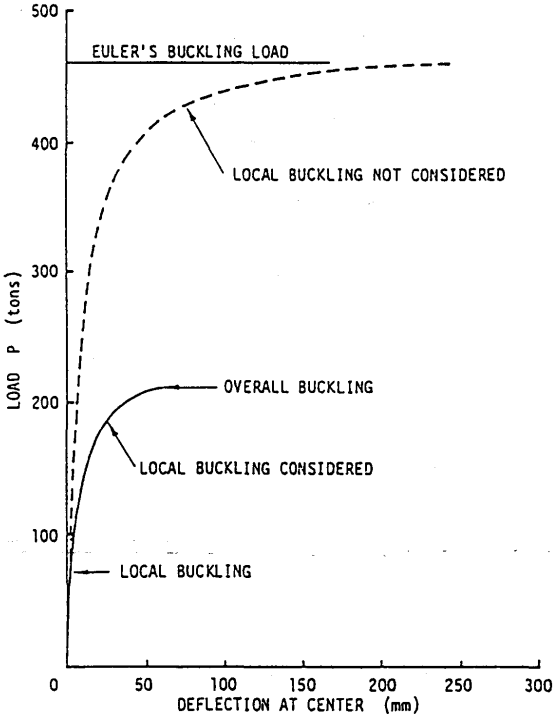

Fig. 14 Load-deflection curves of example box column subjected to axial compression.

buckling load is reduced to one half of the Euler buckling load as shown by the solid lines in Figs. 13 and 14.

Ship Collision Against a Leg of a Jack-up Rig

The energy absorption capacity of a jack-up rig leg in collision is examined. The rig is a three legged platform standing in 75 meters of water. Legs are 104.8 meters in hight and each leg is a K braced lattice structure as shown in **Fig. 15**. Deck weight is 10000 ton and supported on the three legs. A supply boat is assumed to collide with one leg at a point 2 meters below the water line parallel to one face of the leg structure.

In the analysis, considering the inertia of the deck, the leg is assumed to be supported at the deck as well as its lower end as shown in Fig. 15. One third of the deck weight is applied as a soil reaction force at the lower end as shown in the same figure. The collision load is then

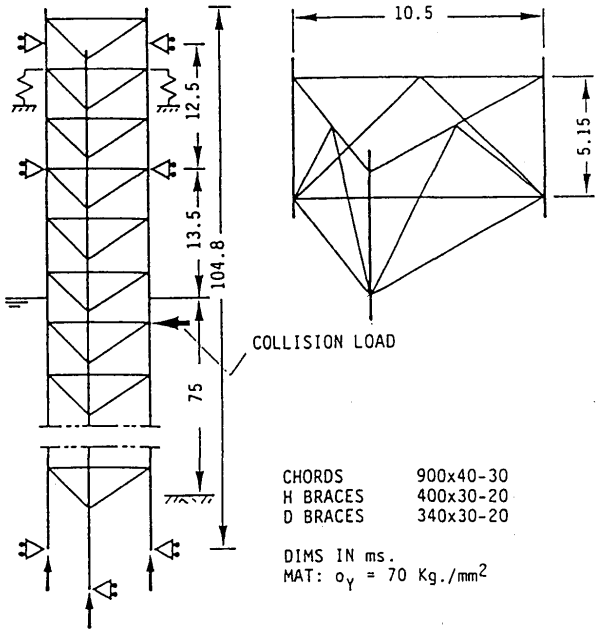

Fig. 15 Leg structure, support conditions and applied load.

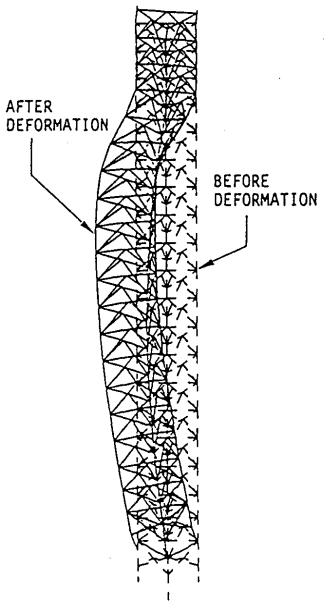

Fig. 16 Deformed shape.

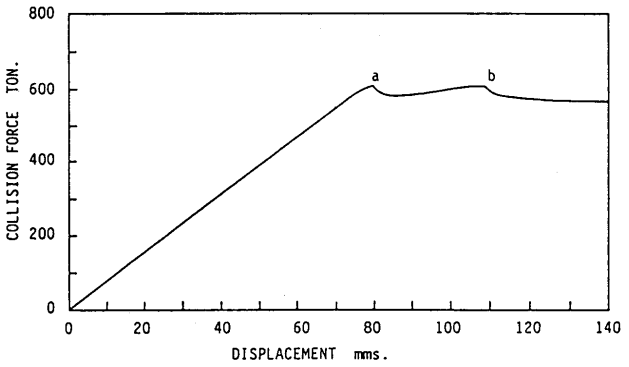

Fig. 17 Load-displacement relationship.

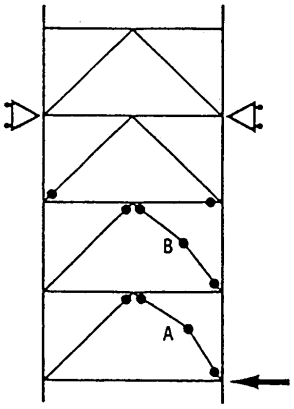

Fig. 18 Colllapse mechanism.

applied incrementally. **Fig. 16** shows the deformed shape of the leg where shear, bending and torsion may be identified. In **Fig. 17** the load is plotted against the horizontal displacement in the direction of the load. Figure 18 shows the location of plastic hinges at the end of the analysis.

On the load-displacement curve in Fig. 17, point a is where brace A shown in **Fig. 18** buckled causing the load to decrease. As other members managed to provide successful redistribution of internal forces, the load increased again and at point b brace B buckled repeating the same phenomenon.

These results indicate that jack-up lattice legs considered in this analysis would undergo a considerable displacement at loads close to ultimate strength thus absorbing a considerable amount of energy.

Ultimate Strength of Hull Girder

Recently Hitachi Zosen has developed a product oil carrier with an intelligent unidirectional girder system and full double shell in the cargo tanks portion of the ship. Order for POCs with this novel structure has been received and two ships delivered. In safety assessment, the capacity of hull girder in vertical bending is evaluated using ISUM. A portion of the hull between two transverse bulkheads, as shown in **Fig. 19**, is considered. Its capacity is calculated in hogging, sagging and under combined bending moment and vertical shearing force. The ISUM model used in the analysis is shown in **Fig. 20**. ISUM plate elements are used to model the outer and inner shell plating, while stiffened plate elements are used to model the girders. Elements with equivalent strength and stiffness are used where manholes exist on the girders. Stiffeners between elements are modeled by beam elements. Due to the high aspect ratio of the plate fields in this design, initial deflections in the same mode as that of buckling is expected to be very small and have negligible effect on the stiffness and the strength of the hull. Residual stresses are partly relieved in tank testing

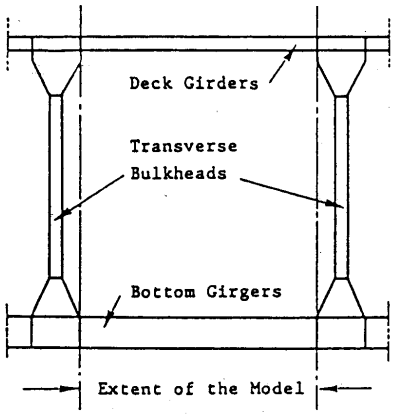

Fig. 19 Extent of ISUM model for capacity evaluation of hull girder.

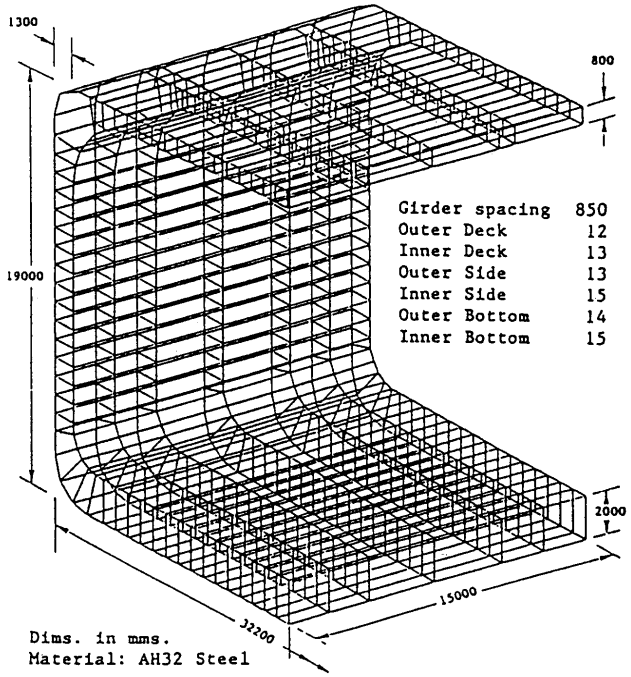

Fig. 20 ISUM model of hull girder for capacity evaluation.

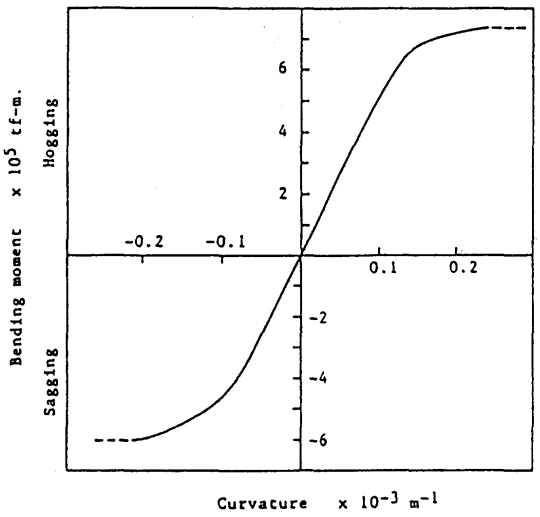

Fig. 21 Moment-curvature relation ship of hull girder at midship.

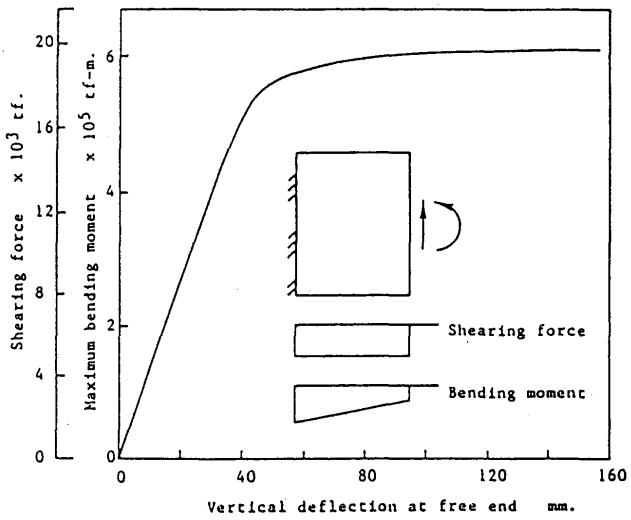

Fig. 22 Load-deflection relationship under combined shearing force and bending moment.

and initial service. Therefore both initial deflection and residual stresses are disregarded in this analysis.

Transverse bulkheads are considered to be stiff enough to be assumed rigid. Therefore, the model has been fixed at one end and fitted with a rigid body on the other end through which the load is applied.

Figure 21 shows the moment-curvature relationship of the hull girder in hogging and sagging.

According to recent reports of ship accidents such as that occurred to Onomichi-maru, jack knifing at foreship section instead of midship section happened to occur. At foreship section, different from midship section, considerable amount of shearing force is specifically acting together with longitudinal bending moment.

Figure 22 shows the relationship between the magnitude of a combined bending and vertical shear load, and the vertical deflection at the free end of the considered hold.

Ultimate Strength of Bottom and Side Girders

Capacities of bottom and side girders of the same POC mentioned in the preceding section above are evaluated using ISUM.

ISUM models used in the analysis are shown in **Fig. 23**. ISUM plate elements are used to model the web plating as well as the inner and outer shells.

Beam elements are used to model the stiffeners. Here also, initial deflection and residual stresses are expected to be very small and have been disregarden in the analysis.

The girders are considered to be restrained against rotation at transverse bulkheads.

Three loads are considered: axial compression, external pressure and internal pressure.

Thirteen load combinations in the ratios shown in **Table 1** are considered. Ultimate strength is also shown in the same table. Results of the analysis have shown that compressive stresses normal to the axes of these girders are small and have negligible effects on their capacity and that capacity may be plotted as an interaction relationship between the axial compressive stress and the net lateral pressure as shown in **Figs. 24** and **25**.

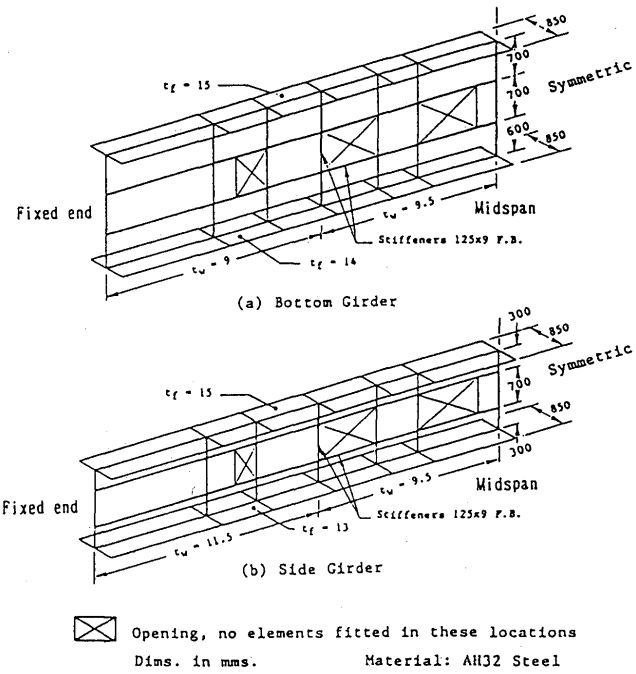

Fig. 23 ISUM model of longitudinal girders.

Table 1 Load combinations applied to longitudinal girders.

Case	σL	q_e	q_l	Ultimate Load Factor ; f_u	
				Bottom Girder	Side Girder
1	1	0.25	0.00	20.25	20.50
2	1	0.25	1.50	19.25	17.75
3	1	0.25	6.00	8.00	6.95
4	1	1.50	0.00	18.25	16.60
5	1	1.50	1.50	21.25	21.50
6	1	1.50	6.00	9.80	8.55
7	1	6.00	0.00	8.20	6.60
8	1	6.00	1.50	10.40	8.55
9	1	6.00	6.00	21.00	22.25
10	1	0.00	3.00	13.50	—
11	1	3.00	0.00	14.00	—
12	1	4.50	0.00	10.60	—
13	1	6.00	3.00	14.00	—

$\sigma L_u = \sigma L \times f_u (kgf/mm^2)$
$q_{eu} = q_e \times f_u (tf/m^2)$
$q_{lu} = q_l \times f_u (tf/m^2)$
$P_u = (q_e - q_l) f_u$

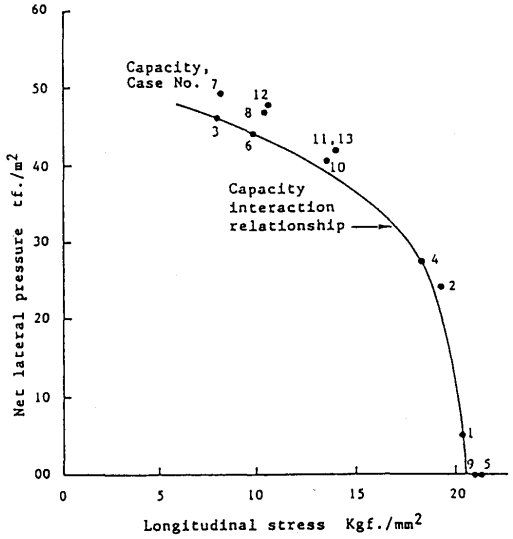

Fig. 24 Capacity interaction relationship of bottom girders.

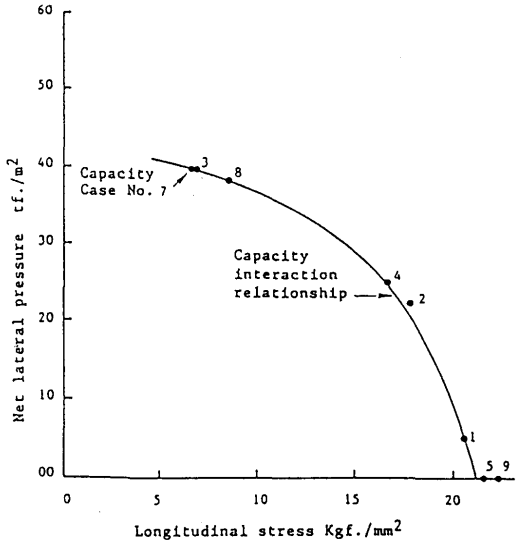

Fig. 25 Capacity interaction relationship of side girders.

Conclusions

From the applications presented in this paper, it may be seen that the number of nodes and elements in ISUM are one or two orders less than those in FEM to analyse the same phenomena. A proportional reduction in modeling time may be expected. Necessary computer time may be from 1/5 to 1/100000 of that required by the finite element method. Accuracy of ISUM is checked and proved to be sufficient for practical use as may be seen in the references indicated above. Plasticity, one major nonlinearity, is accounted for in all ISUM elements by one general method, i.e. the plastic node method. On the other hand, local geometric nonlinearity (within element boundaries), which is another major nonlinearity, is handled differently in each element. A solution to the differential equation for one dimensional element is successfully applied as a deformation function. However, a unified general approach to handle local geometric nonlinearity is highly required to make systematic development of new elements. Finally, the authors express their thanks to Hitachi Zosen LTD. for granting the publication of some of the examples presented in this paper.

References

1. Ueda, Y. and Rashed, S.M.H., "An Ultimate Transverse Strength Analysis of Ship Structures", *Journal of the Society of Naval Architects of Japan,* Vol.136, 1974 (In Japanese).
2. Ueda, Y. and Rashed, S.M.H., "The Idealized Structural Unit Method and Its Application to Deep Girder Structures", *Computer and Structures,* Vol.18, 1984.
3. Ueda, Y., Rashed, S.M.H. and Nakacho, K., "New Efficient and Accurate Method of Nonlinear Analysis of Offshore Tubular Frames (The Idealized Structural Unit Method)", *Jl. of Energy Resources Technology,* ASME, Vol.107, 1985.
4. Ueda, Y., Rashed, S.M.H. and Nakacho, K., "An Improved Joint Model and Equations for Flexibility of Tubular Joints", *Proc. of 6th Int. OMAE Symp.,* 1987.
5. Ueda, Y., Rashed, S.M.H. and Paik, J. K, "Plate and Stiffened Plate Units of the Idealized Structural Unit Method (1st Report)", *Jl of Soc. of Naval Architects of Japan,* Vol.156, 1984 (In Japanese).
6. Ueda, Y., Rashed, S.M.H. and Paik, J. K, "Plate and Stiffened Plate Units of the Idealized Structural Unit Method (2st Report)", *Jl of Soc. of Naval Architects of Japan,* Vol.159, 1984 (In Japanese).
7. Ueda, Y. and Rashed, S.M.H., "Behavior of Damaged Tubular Structural Members", *Jl of Energy Resources Technology,* ASME, Vol.107, 1985.

8. Yao, T., Fujikubo, M. and Bai, Y., "Influence of Local Buckling on Behaviour of Tubular members", *Proc. PRADS,* Vol.2, 1989.
9. Hori, T., Sekihama, M., Rashed, S.M.H., "Structural Design by Analysis Approach Applied to a Product Oil Carrier with a Unidirectional Girder System", *T. RINA,* 1990.
10. Yuhara, T. and Kawamoto, Y., "Numerical Simulation of Ultimate Strength of Ship Structures", *15th SNAJ Summer Symposium (New Naval Architicture),* Sept. 1989 (In Japanese).
11. Ueda, Y. et al., "Ultimate Strength Analysis of Double Bottom Structures in Stranding Conditions", *Proc. of the 3rd Int. Sym. on Practical Design of Ships and Mobile Units,* Tronheim, 1987.
12. Ueda, Y., Rashed, S.M.H. and Naser, Y., "Collision Resistance of Double Sided Vessels", *Report MHI,* 1989 (Restricted).
13. Rashed, S.M.H., Ishihama, T., Nakacho, K. and Ueda, Y., "Ultimate Strength of Jack-Up Rigs in Survival and Punch-Through Conditions" *Proc. of the 3rd Int. Sym. on Practical Design of ships and Mobile Units,* Tronheim, 1987.
14. Moan, T., Amdaho, J., Engseth, A.G. and Granli, T., "Collapse Behavior of Truss Work Steel Platforms", *Boss' 85,* 1985.
15. Kavlie, D. and Soreide, T., "Practical Design in Shipbuilding, Tokyo/Seoul, 1983.
16. Rashed, S.M.H., "Collision Resistance of Offshore Collision Barriers", *Report to Japan Steel Corp.,* 1989 (Restricted).
17. Ueda, Y. et al., "A New Theory on Elastic-Plastic Analysis of Framed Structures", *Technology Reports of Osaka University,* Vol.19, 1969. Ueda, Y. and Yao, T., "The Plastic Node method: A New Method of Plastic Analysis", *Computer methods in Applied mechanics and Engineering,* Vol.34, 1982.
18. Ueda, Y. and Fujikubo, M., "Plastic Node Method Considering Strain-hardening Effects", *Jl of Soc. of naval Architects of Japan,* Vol.160, 1986 (In Japanese).
19. Chen, W.F. and Atsuta, T., *Theory of Beam-Columns,* Vol.1, McGraw-hill Inc., 1976.
20. Selberg, A., *Steel Structures,* (in Norwegian), Tapir, Norway, 1972. Ueda, Y., Rashed, S.M.H., Paik, J.K. and Masaoka, K., "The Idealized Structural Unit Method Including Global Nonlinearities", *J. SNAJ,* June 1986 (in Japanese).